Tropical Water Vapor and Cloud Feedbacks in Climate Models: A Further Assessment Using Coupled Simulations

De-Zheng Sun[1], Yongqiang Yu[2], Tao Zhang[1]

1. Cooperative Institute for Environmental Studies/University of Colorado &NOAA/Earth System Research Laboratory, Boulder, Colorado, USA.
2. LASG, Institute of Atmospheric Physics, Chinese Academy of Sciences, Beijing, China.

July 7, 2008

Corresponding Author Address:
Dr. De-Zheng Sun
NOAA/ESRL/PSD/PSD1
325 Broadway
Boulder, Colorado 80305-3337
Email: dezheng.sun@noaa.gov

Submitted to J. Climate

ABSTRACT:

By comparing the response of clouds and water vapor to ENSO forcing in nature with that in AMIP simulations by some leading climate models, an earlier evaluation of tropical cloud and water vapor feedbacks has revealed two common biases in the models: (1) an underestimate of the strength of the negative cloud albedo feedback and (2) an overestimate of the positive feedback from the greenhouse effect of water vapor. Extending the same analysis to the fully coupled simulations of these models as well as other IPCC coupled models, we find that these two biases persist. Relative to the earlier estimates from AMIP simulations, the overestimate of the positive feedback from water vapor is alleviated somewhat for most of the coupled simulations. Improvements in the simulation of the cloud albedo feedback are only found in the models whose AMIP runs suggest a positive or nearly positive cloud albedo feedback. The strength of the negative cloud albedo feedback in all other models is found to be substantially weaker than that estimated from the corresponding AMIP simulations. Consequently, although additional models are found to have a cloud albedo feedback in their AMIP simulations that is as strong as in the observations, all coupled simulations analyzed in this study have a weaker negative feedback from the cloud albedo and therefore a weaker negative feedback from the net surface heating than that indicated in observations. The weakening in the cloud albedo feedback is apparently linked to a reduced response of deep convection over the equatorial Pacific which is in turn linked to the excessive cold-tongue in the mean climate of these models. The results highlight that the feedbacks of water vapor and clouds—the cloud albedo feedback in particular—may depend on the mean intensity of the hydrological cycle. We have also examined whether the inter-model variations in the feedback from cloud albedo (water vapor) in the ENSO variability are correlated with the inter-model variations of the feedback from cloud albedo (water vapor) in global warming. While we find a weak positive correlation between the inter-model variations in the feedback of water vapor during ENSO and the inter-model variations in the water vapor feedback during global warming, we find no significant correlation between the inter-model variations in the cloud albedo feedback during ENSO and the inter-model variations in the cloud albedo feedback during global warming. The results suggest that the two common biases revealed in the simulated ENSO variability may not be necessarily carried over to the simulated global warming. These biases, however, highlight the continuing difficulty that models have to simulate accurately the feedbacks of water vapor and clouds on a time-scale we have observations.

1. Introduction:

Water vapor provides most of the greenhouse effect of the Earth's atmosphere. Clouds are a major contributor to the planetary albedo (Kiehl and Trenberth 1997). A small change in these radiative effects of water vapor and clouds can either offset or greatly amplify the perturbation to the Earth's radiation balance from anthropogenic effects (Houghton et al. 2001). Therefore, it is imperative for climate models on which our economical polices are increasingly relying on to narrow the uncertainties in their simulations of the feedbacks from water vapor and clouds. Toward that objective, we have to critically evaluate how well the existing leading climate models simulate the feedbacks from water vapor and clouds.

Two methods have been employed to shed insight onto the question how well climate models simulate the feedbacks from water vapor and clouds. The first one is to check the differences in the feedbacks of water vapor and clouds in global warming among different models. A pioneering study using this method was carried out by Cess et al. (1990, 1996). Their analysis revealed that the cloud feedbacks differ greatly among models while the globally averaged feedback from water vapor in the models follows that of a constant relative humidity model. A later study by Soden and Held (2006) reached the same conclusion for the IPCC AR4 models (Meehl et al. 2007). These results underscore the uncertainties in the cloud feedbacks in the climate models, but do not address the question which model has the right cloud feedbacks. Another limitation of these results is that consistency in the simulation of water vapor feedback does not rule out the possibility that all the models have a biased water vapor feedback.

The second method is to compare the response of water vapor and clouds to SST changes over the time scales for which observational data are available. A frequently used natural signal in the SST is El Nino warming (Sun and Held 1996, Soden 1997, Held and Soden 2000, Sun et al. 2006). By comparing the observed changes in the water vapor and clouds with those from the model with the observed SST boundary conditions (AMIP simulations), these studies suggest that the sign of the water vapor feedback in the GCMs is probably correct on the time-scale of ENSO, even when averaged over the entire tropics. The study of Sun et al. (2006) shows, however, that models tend to overestimate the positive feedback of water vapor over the immediate region of the El Nino warming. The study of Zhang and Sun (2008) further shows that at least for the NCAR models, the overestimate of the positive feedback of water vapor during El Nino warming is due to an excessive response of upper tropospheric water vapor to the surface warming. A more serious concern raised by the study of Sun et al. (2006) is the finding of a common bias in the simulation of the cloud albedo feedback in the leading climate models: with the exception of the GFDL model, all the models they analyzed in that study underestimate the response of cloud albedo to the surface warming. Nonetheless, the finding that at least the GFDL model may have a cloud albedo feedback as strong as the observed strikes an optimistic tone.

The study of Sun et al. (2006) used the AMIP simulations. Using AMIP simulations of these models to estimate feedbacks has an inherent limitation: the feedbacks are the feedbacks operating in the immediate neighborhood of the observed climatology. As the mean climate is free to drift to the state that is in turn determined by the feedbacks, the feedbacks may change in the process of integration of the coupled model. In other words, if the coupled system—the models of it in particular—is not strictly a linear feedback system, and if the SST of the equilibrium state of the coupled run differs significantly from the observed, the feedbacks estimated about the equilibrium state of the coupled runs could be significantly different from those estimated from the

corresponding AMIP runs. The coupled models do have a significantly different climatological SST from the observed—they all have an excessive cold-tongue in the equatorial central Pacific (Sun et al. 2006). The purpose of this paper is to further assess the feedbacks from water vapor and clouds over the tropical Pacific region by directly using the outputs from fully coupled runs, and to highlight the impact of the excessive cold-tongue in the coupled models on the feedbacks of water vapor and clouds over that region. Lin (2007) recently examined the cloud albedo feedback over the same region using the shortwave forcing of clouds at the surface, but he did not examine the water vapor feedback. Also, in his calculation of the feedback from the short-wave forcing of clouds at the surface, he did not separate the seasonal signal from the interannual signal. Nor is it clear whether the temporal variations are separated from the regional variations in his calculation. This mixing together variability of different origins make interpretation of the results more challenging. Another important study that is closely related to the present effort is by Bony and Dufresne (2005). Using monthly mean mid tropospheric vertical velocity, they first decomposed the tropical circulations into a series of dynamical regimes and then examined the sensitivity of the cloud forcing in these regimes to a change in local SST. They highlighted the importance of boundary layer clouds by noting that the response of these clouds to a change in local SST in the model simulations of the present climate disagree most with observations. The present effort is focused on the response of the clouds and water vapor over the central and eastern equatorial Pacific to El Nino warming. We will show that even over the region where the peak El Nino warming takes place, models have systematic biases in the simulated feedbacks from water vapor and clouds.

A more difficult question to address is then whether the biases in the water vapor and cloud feedbacks shown up in the ENSO variability in the models will be carried over to the feedbacks of water vapor and clouds in the simulated global warming. To shed some light on this question, we take note that there are significant variations among different models in the simulated feedbacks of

water vapor and clouds on both time scales—ENSO and global warming. If the model that has the weakest cloud albedo feedback during its simulated ENSO variability is also the model which has the weakest cloud albedo feedback in its simulated global warming, and more generally the variations in this feedback simulated by different models are strongly positively correlated on these two time-scales—ENSO variability and global warming, we may have a piece of evidence in hand to support a positive connection between biases in the cloud albedo feedback on these two different time-scales. Conversely, if no such a strong positive correlations are found, we may conclude that the feedbacks in ENSO are not a harbinger of the feedbacks in global warming. So we will examine whether variations among the models in the feedbacks during ENSO and during global warming have significant correlations. The issue whether the feedbacks on these two different time-scales are linked has been addressed to some degree and from a different angle by Bony and Dufresne (2005) and Zhu et al. (2007). Bony and Dufresne (2005) compared the interannual feedbacks with climate feedbacks. They noted that the large inter-model differences in the feedback in the simulated global change in their weakly subsiding case are not presented in the feedback in the interannual variability. Zhu et al. (2007) showed that changes in the low cloud amount in response to the 1997-98 El Nino are different from the changes in the low cloud amount in response to simulated global warming. The former is more linked to the changes in position of the convective activities while the latter is more linked to a change in the vertical stability.

The paper is organized as follows. The methodology is briefly described in section 2. In section 3, we first report the estimates of the feedbacks of water vapor and clouds in ENSO variability using the coupled runs of those models analyzed in Sun et al. (2006). These coupled runs are control runs. We then do the same feedback analysis using the 20th century simulations by an expanded group of models from the IPCC AR4 archive (Meehl et al. 2007). We will see that the bias in the cloud albedo feedback and the bias in the water vapor feedback identified in Sun et al. (2006) exist in all

these coupled simulations—control runs of the original group as well as these 20th century simulations runs of the expanded group of models. In section 4, we will attempt to address the question whether the variations among models in the simulated cloud and water vapor feedbacks in ENSO variability are correlated with variations in the feedbacks of water vapor and clouds in global warming. Summary and conclusions are provided in section 5.

2. Methodology

In estimating the feedbacks of water vapor and clouds in the ENSO cycle, we will follow Sun et al. (2006): we will use the response of tropical convection to ENSO forcing to obtain the feedbacks of water vapor and clouds associated with tropical convection. We will first analyze the group of coupled models whose AMIP runs we analyzed in the study of Sun et al. 2006. In that study, we examined nine AGCMs. Seven of the nine AGCMs have a corresponding fully coupled GCM whose control runs are available for our analysis. These models are: NCAR CCSM1 (Boville and Gent 1998), the NCAR CCSM2 (Kiehl and Gent 2004), the NCAR CCSM3 at respectively T42 and T85 resolution (Collins et al. 2006, www.ccsm.ucar.edu/experiments/ccsm3.0/), the HadCM3 (Collins et al. 2001), the French IPSL CM4 model (Marti et al. 2005), and the GFDL CM2.0 (Delworth et al. 2006). Unless explicitly stated, calculations for this group models use a 50 year-long segment of the control runs of the models.

We then extend the analysis to a larger set of coupled models using the 20th century simulations submitted to CMIP3 (Meehl et al. 2007) by various groups (http://www-pcmdi.llnl.gov/ipcc/model_documentation/ipcc_model_documentation.php). We limit our analysis to those models that do not use flux adjustment. In the AR4 archive, there are 17 models that do not use flux adjustment, but only 13 of them have all the variables we need to compute the

feedbacks from water vapor and clouds. After excluding one more model from these 13 models because the interannual variability in the cold-tongue SST in this model is too weak to be used to calculate the feedbacks, we end up with an expanded group of 12 models. These models are the France CNRM CM3, the US GFDL2.0, the US GFDL2.1, the US GISS Model_e_h, the China IAP-FGOALS, the France IPSL-CM4, the Japan MIROC 3.2 (medres), the Japan MIROC 3.2 (hires), the German ECHAM5/MPI, the US NCAR CCSM3, the UK HadCM3, and the UK HadGEM1. Details for each of these models, including the spatial resolutions for the atmosphere and ocean components of these models, can be viewed on the aforementioned web page.

3. Feedbacks in the ENSO cycle

Applying the same linear regression technique of Sun et al. (2006) to the simulations of tropical inter-annual variations by those coupled models, we obtain Table 1. The numbers in the parenthesis are the results from the corresponding AMIP runs that are available for us. The observational results listed in the table are obtained using the dataset by Zhang et al. 2004. This dataset is based on ISCCP data (Rossow and Schiffer 1999) and covers a much longer period than the 4 year long ERBE period used in Sun et al. (2006). The estimate of the feedbacks from the greenhouse effect of water vapor clouds from the ISCCP data are quite close to those from ERBE. The estimate of the negative feedback from the short-wave forcing from this extended period covered by ISCCP data is significantly larger than that estimated from ERBE—about -14 $W/M^2/K$ from ISCCP versus -11 $W/M^2/K$ from ERBE. Over the period these two data sets overlap (i.e., the ERBE period), the feedback from the short-wave forcing estimated from ISCCP data is -12.5 $W/M^{2/}$ K. So only part of the difference~1.5 $W/M^{2/}$ K. is due to the length of the data used. Note that the short-wave forcing from ISCCP is derived from a radiation model constrained by ISCCP observations. Exact agreement between ISCCP data and the ERBE period is not guaranteed. It is probably safe to

assume that the feedback from the short-wave forcing of clouds is between -11 $W/M^{2/}$ K and -14 $W/M^{2/}$ K.

The problems uncovered in the previous analysis also show up in this extended analysis. First, models tend to underestimate the strength of the negative feedback from cloud albedo. This is true whether one uses the estimate from ERBE or from the estimate from ISCCP. The model that now has the strongest negative cloud albedo feedback is the IPSL/CM4, but the feedback is only of 50%-70% of the estimate from the observations. Compared to the corresponding value estimated from their AMIP runs, substantial weakening in the simulated strength of the cloud albedo feedback occurs in all the four models that were identified as better models in the previous analysis using their AMIP runs (the NCAR Model at T85, the UK model, the French Model, and the GFDL model). This reduction in the strength of the cloud albedo feedback is particularly notable for the GFDL model—the value changed from -15.43 $Wm^{-2}K^{-1}$ –the value estimated from the AMIP run—to -6.14 $Wm^{-2}K^{-1}$ –the value estimated from the coupled run.

Fig. 1 and Fig. 2 provide respectively a basin-wide view of the response of C_s to El Nino warming in the coupled models and in their corresponding AMIP runs. Using the data from Zhang et al. 2004 results in a pattern for the observations that is very similar to that from the ERBE data---a negative response of Cs in the central and eastern Pacific is flanked by a positive response in the western Pacific, the Southern Pacific Convergence Zone, and in the north subtropical Pacific. The positive response in the north subtropical Pacific is consistent with the finding by Bony and Dufresne (2005). Except in the region immediately adjacent to the east coast and slightly off equator, observations (Fig.1a and Fig.2a) do not show a positive feedback from C_s in the far eastern equatorial Pacific (5^oS-5^oN). A positive feedback from C_s in the far equatorial eastern Pacific was noted in Lin (2007) who used the same dataset as the present study, but had the seasonal cycle

included in his calculation of the feedback from C_s. The absence of this feature in our calculation suggests that the positive feedback from C_s in the far equatorial eastern Pacific found in the study of Lin (2007) is from the seasonal cycle. Interestingly, many models do have a positive feedback on the ENSO time-scale in the far equatorial eastern Pacific.

The spatial pattern of the response of C_s in the coupled models resembles that obtained from their corresponding AMIP runs, but the maximum response of C_s is located more westward in the coupled models by about 20^o. With the exception of NCAR CCSM2 and CCSM3 at T42, the maximum response of C_s in the coupled simulations is also weaker than that in the corresponding AMIP runs. In the AMIP runs, the maximum response of Cs in NCAR CCSM3 at T85, UKMO/HadCM3, IPSL/CM4, and GFDL/CM2.0 has a value that exceeds -30 $Wm^{-2}K^{-1}$. In their corresponding coupled runs, however, the maximum response of C_s in these four better models is significantly reduced. The reduction in the maximum response of C_s in NCAR CCSM3 at T85, IPSL/CM4, and GFDL/CM2.0 is about 10 $Wm^{-2}K^{-1}$. The reduction in the maximum response of C_s in UKMO/HadCM3 is even higher (~15 $Wm^{-2}K^{-1}$).

There are exceptions to this general weakening in the response of C_s --NCAR CCSM2 and NCAR CCSM3 at T42. NCAR CCSM2 has hardly any negative response in its AMIP run, but now develops a substantially negative response in the region immediately west to the dateline (150^oE-170^oE). The improvements in NCAR CCSM3 at T42 are even more substantial. The response of C_s in this model is comparable to that in GFDL/CM2.0. Such a "self-correction" of the cloud albedo feedback clearly indicates the importance of nonlinearity in the coupling between the atmosphere and ocean. While it is encouraging to see that ocean-atmosphere coupling allows a "self-correction" to take place, it is disappointing to see that this "self-correction" is limited to the two models whose cloud albedo feedback assessed from their AMIP runs (i.e., about the observed SST as AMIP runs

use the observed SST as the boundary forcing) has the largest error. As indicated by the results from their AMIP runs, the negative feedback from cloud albedo barely exists in these two models in the immediate neighborhood of the observed SST (see the numbers in the parenthesis). All other models that have been judged from their respective AMIP runs to have a significantly negative feedback of cloud albedo at the observed SST are found to have an even weaker cloud albedo feedback at their respective equilibrium SST.

The general weakening of the response of C_s in the coupled models (relative to the values estimated from the AMIP runs) is linked to the weakened precipitation response. Fig. 3 and Fig. 4 show respectively the precipitation response to El Nino warming in the coupled models and in the corresponding AMIP runs. Contrasting Fig. 3 with Fig. 4, one finds that the reduction in the maximum response of the precipitation in NCAR CCSM3 at T85, UKMO/HadCM3, IPSL/CM4, and GFDL/CM2.0 all exceeds 30%. The location of the maximum response of precipitation in these coupled models also shifts westward relative to that in the AMIP runs. The general reduction in the precipitation and the westward shift of the response suggest that the excessive cold-tongue in these models plays a role in further weakening the response of C_s to SST changes in that region. Lin (2007) also noted that coupling shifts the deep convection westward and results in a reduction in the precipitation over the equatorial Pacific. (Interestingly, the two models (NCAR CCSM2 and CCSM3 at T42) that have an improved cloud albedo feedback are the only two models that do not have a significant weakening in their maximum response in the precipitation).

To further examine the suggestion that the weakened precipitation response over the cold-tongue region is a cause of the weakened response in the short-wave forcing of clouds, we plotted the scatter diagram of precipitation and SST over the cold-tongue region (Fig5a). The figure shows that about their respective climatology (i.e., near the zero point as what are plotted here), the

precipitation increases with SST increases at a faster rate in the observations than that in the models. Only when the positive SST anomalies are very large, does the rate of increase of precipitation with respect to SST in some models becomes comparable to that in the observations. The corresponding figure for the surface level solar radiation shows that the relationship between the surface solar radiation and SST mirrors the relationship between precipitation and SST (Fig.5b). About its respective climatology, the surface solar radiation decreases at a faster rate in the observations than in the models.

The new estimates also confirm another common bias existing in the climate models: the overestimate of the positive feedback of water vapor. Comparing the estimates from the coupled runs with those from the corresponding AMIP runs reveals that estimating from their AMIP runs of the climate models can result in a stronger positive feedback of water vapor. For example, the new estimate of the water vapor feedback in the UKMO/HadCM3 is now significantly closer to the observed value than that from its AMIP runs. Still, all the models have a stronger water vapor feedback than that indicated in observations. The overestimate ranges from about 25% in NCAR CCSM2 to about 45% in NCAR CCSM3 and IPSL/CM4. Discrepancies of this magnitude cannot be accounted for by errors in the observations. In any case, the existence of a significant spread in this discrepancy among these models suggests that any agreement in the global averaged values in this regard must be linked to error cancellations among different regions. Fig. 6 shows the spatial pattern of the response of G_a. Clearly, the models do not just differ from the observations over the immediate region of surface warming due to El Nino, they also differ in the surrounding regions—the far western Pacific and the subtropical regions. Fig. 7 shows the pattern of Ga from the corresponding AMIP runs. Comparing the spatial pattern of G_a in these two figures indicate a westward shift of convection in the coupled models relative to their AMIP runs.

With the exception of the NCAR CCSM2 and CCSM3, the estimates using the coupled simulations also yield a lower value for the positive feedback from the greenhouse effect of clouds than from the corresponding AMIP runs. The decrease in the strength of the positive feedback from the greenhouse effect of clouds is consistent with the decrease in the strength of the negative feedback from the cloud albedo. The exceptional behavior in the two NCAR models in this regard is also consistent with the exceptional behavior in these two models in simulating the cloud albedo feedback (recall that the feedback from cloud albedo in these two models is estimated to be more negative than that estimated from AMIP runs). Fig. 8 and Fig. 9 show respectively the spatial pattern of the response of the greenhouse effect of clouds (C_l) in the coupled and the AMIP simulations of the models. The contribution to the increase in the value of $\frac{\partial}{\partial T} C_l$ as shown in Table 1 in CCSM2 and CCSM3 mainly comes from the western edge of the equatorial cold-tongue region defined here (150^{o}E-250^{o}E). Judging from Fig.8 and the corresponding pattern of the precipitation response (Fig. 3), it is likely that the large positive initial bias in the cloud albedo feedback—the bias shown up in the corresponding AMIP runs--in these two models enhances the deep convection in the region about 150 ^{o}E-170^{o}E (where SST is already warm) to a degree that the weakening effect from the excessive cold-tongue is offset.

Although the estimates from the coupled simulations yield a lower value of the feedback from C_l for the majority of the models, the lack of cancellation between the feedback from C_l and the feedback from C_s in the models, as first revealed in the estimates from the AMIP runs, continues to exist in the estimates from the coupled simulations because of the larger bias in the feedback from Cs in the new estimates. Column 5 of Table I lists the net clouds feedback (C_l+ $C_{s)}$. In the observations, the net cloud feedback is slightly negative. All the models, judging from the estimates from the coupled simulations at least, have a positive net cloud feedback. The relationship between Cs and Cl in the models is biased. In contrast, not all the models overestimate the feedback from the total greenhouse

effect of water vapor and clouds (G_a+ C_l) (Column 3, Table 1). Two of the models are actually found to underestimate the combined feedback from G_a and C_l (The NCAR CCSM2 and the UKMO/HadCM3). Clearly, the relationship between G_a and C_l is not the same in all the models.

As in Sun et al. (2006), we also assess the corresponding feedback from the atmospheric transport and deduce the feedback from the net surface heating from the energy balance equation of the atmosphere. We derive the net surface heat flux by combing the latent and sensible heat fluxes from NCEP with the radiative fluxes from ISCCP. All the models underestimate the negative feedback from the net surface heat flux. All the models in the table also underestimate the negative feedback from the atmospheric transport. Seen in the net atmospheric feedback ($\frac{\partial F_a}{\partial T}$) and the feedback from the net surface heating ($\frac{\partial F_s}{\partial T}$), the discrepancy with the observations in the new estimates increases in the models that were identified as better models in this regard in the previous analysis (GFDL CM2, IPSL/CM4, HadAM3, and NCAR CAM3-T85), but decreases in the models that were identified as the worse models in this regard (NCAR CAM1, NCAR CAM2, and NCAR CAM3). Still, no models in the new estimates have a regulatory effect that is comparable to the observations. The best model identified in the previous analysis—the GFDL/CM2, however, remains the one that has the strongest the regulatory effect, though the new estimate suggests that this regulatory effect from deep convection in this model is still too weak compared to observations (about -10$Wm^{-2}K^{-1}$ in the model versus about -22 $Wm^{-2}K^{-1}$)

We have also extended the analysis to more models by using the 20th century simulations submitted to the CMIP3 archive by various modeling centers (Meehl et al. 2007). We limit our analysis here only to those models that do not use flux adjustment and have all the variables we need in the archive. We then eliminate one model that does not have a significant ENSO signal. This comes

down to 12 models for our extended analysis. The results are summarized in Table 2. The numbers in the parentheses are the corresponding feedbacks from the AMIP runs of these 12 models. (Note that not all these models have an AMIP run or have a complete set of variables from the AMIP runs). Judging from the estimates from the coupled simulations, all the models listed in Table II have a weaker cloud albedo feedback than what is seen in observations. Again, we see that the estimates using coupled simulations of ENSO result in a weaker cloud albedo feedback than that estimated from the corresponding AMIP simulations. Note that judging alone from the estimates from the AMIP simulations of this extended list of models, three models actually have a stronger cloud albedo feedback than what is seen in the observations. Still, most of the models already have a weaker cloud albedo feedback than observations in their AMIP simulations. All the listed models in Table II with the exception of the UKMO-HadGEM1, also overestimate the feedback from water vapor. So the two common biases identified in our earlier analysis are in fact prevalent among the coupled models. Regression maps like Fig. 3 and Fig. 4 for these models again show a weakened and more westward shift of the precipitation response in these coupled models than in their corresponding AMIP runs (not shown here to avoid redundancy).

4. Can feedbacks in ENSO be harbingers of the feedbacks in global warming?

The above analysis establishes that there are common biases in the simulated feedbacks in the ENSO cycle: models tend to underestimate the negative feedback from cloud albedo, and over estimate the positive feedback from water vapor. The question is then whether these systematic biases will be carried over to the global warming simulations. To address this question, we examine whether variations in the feedbacks during global warming among different models are correlated with the variations in the same feedbacks during the ENSO cycle among these models. In other words, we examine whether the models that have a stronger feedback in ENSO than their peer

models also tend to have a stronger feedback in global warming than their peer models. We have estimated the feedbacks in the global warming using the A1B scenario runs by computing the linear trends of the SST, the cloud short-wave forcing, and the greenhouse effect of water vapor over 2000---2100. We then obtain the feedback of cloud albedo as the ratio between the trend of the shortwave cloud forcing and the trend of the SST, and the feedback of water vapor as the ratio between the trend of the greenhouse effect of water vapor over the trend of SST. Fig. 10a is a scatter diagram showing the variations in the cloud albedo feedback in global warming among models (the vertical axis) over the cold-tongue region against the variations in the same feedback in the ENSO cycle over the same region (the horizontal axis). The figure shows that there are no correlations between the variations on these two different time-scales. The CNRM-CM3 has the strongest negative feedback of cloud albedo in the ENSO cycle, but has almost the weakest negative feedback of cloud albedo in global warming. For the feedback from the greenhouse effect of water vapor, there is some correlation between the variations among model-simulated feedback in global warming and the variations among the model simulated feedback in the ENSO cycle (Fig. 10b), but the correlation is not strong (about 0.57). Although the models that have a relatively weaker feedback of water vapor generally line up (e.g., UKMO-HadGEM1, MIRO3.2 (medres), and MIRO3.2 (nires)), the models that have a relatively stronger water vapor feedback do not. The model that has the strongest water vapor feedback during ENSO is the IPSL-CM4, but this model does not have the strongest feedback in the global warming (in fact, measured by the strength of the feedback during global warming, it only ranks as the 8^{th}.)

We have also computed a global mean cloud albedo feedback—the ratio between the trend in the short-wave cloud forcing averaged over the global oceans and the trend in the global mean SST. Variations in this feedback among the models are not correlated with the variations in the feedback during the ENSO cycle over the cold-tongue region (Fig. 11a). This is also true for the relationship

between the global mean water vapor feedback during global warming and the regional water vapor feedback over the cold-tongue in the ENSO cycle (Fig. 11b).

These results suggest that at least in the models, the feedbacks of water vapor and clouds estimated from the ENSO cycle cannot be used as harbingers for the feedbacks of water vapor and clouds during global warming.

5. **Conclusion.**

The extended calculation using coupled runs confirms the earlier inference from the AMIP runs that underestimating the negative feedback from cloud albedo and overestimating the positive feedback from the greenhouse effect of water vapor over the tropical Pacific during ENSO is a prevalent problem of climate models. The estimates from the coupled simulations of both the cloud albedo feedback and the water vapor feedback differ from the estimates from the corresponding AMIP simulations. The changes in the cloud albedo feedback are particularly significant. The previous analysis of Sun et al. (2006) has suggested that the GFDL CM2 may have a cloud albedo feedback that is as strong as observations. The new estimate with the coupled runs puts this suggestion in doubt as the new estimate is significantly weaker than the previous estimate. All models we have examined in this analysis are found to have a weaker negative feedback from the net surface heating than that from observations, indicating that deep convection over the equatorial Pacific in the models has a weaker regulatory effect over the SST in that region. The differences between the values estimated from the coupled runs and the values estimated from the corresponding AMIP runs appear to be linked to the excessive cold-tongue in the climatology in the coupled models.

The two common biases, shown in the ENSO cycle, however, do not appear to be carried over the global warming simulations. The variations in the cloud albedo feedback among different models

are not correlated with the variations in the same feedback in the global warming simulations among different models. The variations in the water vapor feedback among different models during ENSO over the cold-tongue are positively correlated with the variations in the water vapor feedback during global warming, but the correlation is weak. There is no correlation between the feedbacks over the cold-tongue region during ENSO and the globally averaged feedbacks during global warming. Therefore, the overestimate of the water vapor feedback and the underestimate of the cloud albedo feedback during the ENSO cycle in the models do not necessarily imply that the sensitivity of the mean tropical climate to anthropogenic forcing is overestimated by the models. As noted by Zhu et al. (2007) in two leading GCMs that the changes in the cloud amount in response to ENSO and to global warming may involve different mechanisms. On the other hand, we are not suggesting that the prevalence of these two biases in the models during ENSO should not be of concern for the accuracy of global warming simulated by the models. This is because the lack of correlation in the models between the feedbacks on these two time-scales could also be due to error cancellations in the models. Conversely, the lack of the spread among models in the simulated interannual feedbacks does not guarantee that the inter-model differences in the corresponding climate feedbacks are not large (Bony and Dufresne 2005). In any case, the present results highlight the continuing difficulty that models have in simulating accurately the water vapor and cloud feedbacks in the deep tropics on the time-scale over which we have observations to compare with model simulations. The results should also be of value to the diagnosis of the causes of the biases in the ENSO amplitude in the models.

Acknowledgement

This research was supported partially by NOAA's office of global programs--the Climate Dynamics Program and Experimental Prediction Program (CDEP), and partially by the NSF Climate Dynamics Program (ATM-9912434, ATM-0332760, and ATM-0553111). Using data from IPCC AR4 models, this work was also partially supported under the auspices of the U.S. Dept. of Energy, Office of Science, at the University of California Lawrence Livermore National Laboratory under Contract W-7405-Eng-48. Dr. Y. Yu was partially supported by a grant from National Science Foundation of China (NSFC-40675049) and a grant from the National Basic Research Program of China (2007CB411806). We are grateful to the editor Dr. Anthony D. Del Genio, and to the two anonymous reviewers, for their comments and suggestions. We also would like to thank Drs. William Collins, Curt Covey, James Hack, Isaac Held, Jeffrey Kiehl, Steve Klein, Jerry Meehl, and Roger Pielke for their encouragement and advice in this research.

REFERENCES

Barkstrom, B. R., E. F. Harrison, G. L. Smith, R. Green, J. Kibler, R. D. Cess, and the ERBE Science Team,1989: Earth Radiation Budget Experiment (ERBE) Archival and April 1985 Results. *Bull. Amer. Meteor. Soc.,* **70,** 1254 –1262.

Bony, S., and J.-L. Dufresne, 2005: Marine Boundary Layer Clouds at the Heart of Tropical Cloud Feedback Uncertainties in Climate Models. *Geophys. Res. Lett.,* **32,** DOI: 10.1029/2005GL023851.

Boville, B. A., and P. R. Gent, 1998: The NCAR Climate System Model, Version One. *J. Climate,* **11**, 1115-1130.

Cess, R. D., et al, 1990: Intercomparison and interpretation of climate feedback processes in 19 atmospheric general circulation models. *J. Geophys. Res.,* **95**, 16,601-16,615.

Cess, R. D., et al., 1996: Cloud feedback in atmospheric general circulation models: An update. *J. Geophys. Res.,* **101**, 12,791-12,794.

Clement, A., R. Seager, M.A. Cane, and S.E. Zebiak, 1996: An ocean dynamical thermostat. *J. Climate*, **9,** 2190-2196.

Collins, W.D. Maurice L. Blackmon, G. B. Bonan, J. J. Hack, T. B. Henderson, J. T. Kiehl, W. G. Large, D. S. McKenna, C. M. Bitz and C. S. Bretherton, J. A. Carton, P. Chang, and S. C.

Doney, 2006: The Community Climate System Model Version 3 (CCSM3), *J. of Climate*, **19**, 2122–2143.

Collins, M., S.F.B. Tett, and C. Cooper, 2001: The internal climate variability of a HadCM3, a version of the Hadley Centre coupled model without flux adjustments. *Clim. Dyn.,* **17,** 61-81.

Delworth, T. L., A. Rosati, R. J. Stouffer, K. W. Dixon, J. Dunne, K. Findell, P. Ginoux, A. Gnanadesikan, C. T. Gordon, S. M. Griffies, R. Gudgel, M. J. Harrison, I. M. Held, R. S. Hemler, L. W. Horowitz, S. A. Klein, T. R. Knutson, S-J. Lin, P. C. D. Milly, V. Ramaswamy, M. D. Schwarzkopf, J. J. Sirutis, W. F. Stern, M. J. Spelman, M. Winton, A. T. Wittenberg, B. Wyman, et al., 2006: GFDL's CM2 Global Coupled Climate Models. Part I: Formulation and simulation characteristics. *J. Climate*, **19**, 643-674.

Held, I.M., and B. Soden, 2000: Water vapor feedback and global warming. Annual Review of Energy and the Environment, **25**, 441-475

Houghton, J. T., Y. Ding, D. J. Griggs, M. Noguer, P. J. van der Linden, X. Dai, K. Maskel, and C. A. Johnson, Eds., 2001: *Climate Change 2001*: *The Scientific Basis.* Cambridge University Press, 881 pp.

Hourdin, F., I. Musat, S. Bony, P. Braconnot, F. Codron, J.-L. Dufresne, L. Fairhead, M.-A. Filiberti, P. Friedlingstein, J.-Y. Grandpeix, G. Krinner, P. LeVan, Z.-X. Li, F. Lott, 2005: The LMDZ4 general circulation model: climate performance and sensitivity to parametrized physics with emphasis on tropical convection. *Climate Dynamics*, **27**, 787-813.

Kalnay, E. and Coauthors, 1996: The NCEP/NCAR 40-year reanalysis project. *Bull. Amer. Meteror. Soc*., 77, 437-471.

Kiehl, J. T., and P. R. Gent, 2004: The Community Climate System Model, Version Two. J. *Climate,* **17**, 3666-3682.

Kiehl, J. T. and Trenberth, K. E., 1997: Earth's Annual Global Mean Energy Budget. *Bull. Amer. Met. Soc*., **78**, 197-208.

Lin, J.-L., 2007: The Double-ITCZ problem in IPCC AR4 coupled GCMs: Ocean-Atmosphere Feedback Analysis. *J. Climate*, **20**, 4497—4525.

Marti O., P. Braconnot, J. Bellier, R. Benshila,S. Bony, P. Brockmann, P. Cadulle, A. Caubel, S. Denvil, J.L. Dufresne, L. Fairhead, M.-A. Filiberti,T. Fichefet, P. Friedlingstein, J.-Y. Grandpeix, F. Hourdin, G. Krinner, C. Levy, I. Musat, and C. Talandier, 2005: The new IPSL climate system model: IPSLCM4 (http://dods.ipsl.jussieu.fr/omamce/IPSLCM4/DocIPSLCM4/FILES/DocIPSLCM4.pdf)

Meehl, G.A., and Co-Authors, 2007: The WCRP CMIP3 multi-model dataset: A new era in climate change research. . *Bull. Amer. Met. Soc*., *BAMS*, **88**, 1383-1394, DOI: 10.1175/BAMS-88-9-1383

Rossow, W. B., and R. A. Schiffer, 1999: Advances in understanding clouds from ISCCP. *Bull. Amer. Meteor. Soc.,* **80,** 2261–2288.

Rayner, N. A., E. B. Horton, D. E. Parker, C. K. Folland, and R. B. Hackett, 1996: Version 2.2 of

the Global Sea-Ice and Sea Surface Temperature Data Set, 1903–1994. Climate Research Tech. Note 74 (CRTN74), Hadley Centre for Climate Prediction and Research, Met Office, Exeter, Devon, UnitedKingdom, 35 pp.

Sun, D.Z., J. Fasullo, T. Zhang, and A. Roubicek, 2003:On the Radiative and Dynamical Feedbacks over the Equatorial Cold-tongue. *J. Climate,* **16,** 2425-2432.

Sun, D.-Z. and I.M. Held, 1996 : A comparison of modeled and observed relationships between interannual variations of .water vapor and temperature. *J. Climate*, **9**, 665-675.

Sun, D.-Z., T. Zhang, C. Covey,S. Klein, W.D. Collins, J.J. Hack, J.T. Kiehl, G.A. Meehl, I.M. Held, and M. Suarez, 2006 : Radiative and Dynamical Feedbacks Over the Equatorial Cold-tongue: Results from Nine Atmospheric GCMs. *J. Climate,* **19** , 4059-4074.

Soden, Brian J., "Variations in the tropical greenhouse effect during El Nino," *J. Climate*, **10**, 1050-1055, May 1997

Soden, B., and I. Held, 2006: An assessment of climate feedbacks in coupled ocean-atmosphere models. *J. Climate,* **19,** 3354-3360.

Xie, P., and P.A. Arkin, 1996: Analyses of Global Monthly Precipitation Using Gauge Observations, Satellite Estimates, and Numerical Model Predictions. *J. Climate,* **9**, 840-858.

Zhang, T., and D.-Z. Sun, 2008: What Causes the Excessive Response of the Clear-Sky Greenhouse Effect to El Nino Warming in the NCAR Community Atmosphere Models? *J. Geophys. Research*, 113, D02108, doi:10.1029/2007JD009247.

Zhu, P., J.J. Hack, J.T.Kiehl, and C.S. Bretherton, 2007: Climate Sensitivity of Tropical and Subtropical Marine Low Cloud Amount to ENSO and Global Warming due to Doubled CO2. *J. Geophys. Res*., **112**, D17108, doi:10.1029/2006JD008174.

FIGURE CAPTIONS

Figure 1: Response of the short-wave forcing of clouds (Cs) to El Nino warming. Shown are coefficients obtained by linearly regressing Cs at each grid point on the SST averaged over the equatorial Pacific (5^oS-5^oN, 150^oE-250^oE).

Figure 2: Same as Fig.1 but for the corresponding AMIP runs.

Figure 3: Same as Fig.1, but for the precipitation. The precipitation data are from Xie and Arkin (1996).

Figure 4: Same as Figure 3, but for the corresponding AMIP runs

Figure 5: Scatter diagrams showing the relationship between the precipitation and the SST (a) and the relationship between the surface solar radiative heating and the SST (b). Interannual anomalies of these quantities averaged over the equatorial Pacific (5^oS-5^oN, 150^oE-250^oE) and for the period July 1983—December 2001 are used for these figures.

Figure 6: Same as for Fig. 1, but for the greenhouse effect of water vapor (G_a).

Figure 7: Same as for Fig. 6, but from the corresponding AMIP runs.

Figure 8: Same as for Fig. 1, but for the greenhouse effect of clouds (C_l).

Figure 9: Same as for Fig. 8, but for the corresponding AMIP runs.

Figure 10: (a) Correlations between variations among models in the feedback from cloud albedo over the cold-tongue region during ENSO and variations among models in the same feedback during global warming over the same region. (b) Correlations between variations in the feedback from water vapor over the cold-tongue region during ENSO and the variations in the feedback during global warming over the same region. Note that the variations correlated are the variations of the concerned feedback among different models. The feedbacks in global warming were estimated from trends in the projected global warming during 2000—2100 under the A1B scenario. See text for more details.

Figure 11: (a) Correlations between variations among models in the feedback from cloud albedo over the cold-tongue region during ENSO and variations in the same feedback during global warming over the global oceans (b) Correlations between variations among models in the feedback from water vapor over the cold-tongue region during ENSO and variations among models in the same feedback during global warming over the global oceans. The feedbacks in global warming over the global oceans were estimated from trends over the oceanic region in the projected global warming during 2000—2100 under the A1B scenario. See text more details.

TABLE CAPTIONS:

Table I: Tropical water vapor and cloud feedbacks from observations and coupled climate models. $\frac{\partial}{\partial T}G_a$, $\frac{\partial}{\partial T}C_l$, and $\frac{\partial}{\partial T}C_s$ are respectively the water vapor feedback, the feedback from the long-wave forcing of clouds, and the feedback from the short-wave forcing of clouds. The feedback from the atmospheric transport ($\frac{\partial}{\partial T}D_a$), the net atmospheric feedback ($\frac{\partial F_a}{\partial T} = \frac{\partial G_a}{\partial T} + \frac{\partial C_l}{\partial T} + \frac{\partial C_s}{\partial T} + \frac{\partial D_a}{\partial T}$), and the feedback from the net surface heat flux into the ocean ($\frac{\partial}{\partial T}F_s$) are also listed. The values for these feedbacks are obtained through a linear regression using the inter-annual variations of the SST and the corresponding fluxes over the equatorial Pacific (5^{o}S-5^{o}N, 150^{o}E-250^{o}E). The observational results for the water vapor and cloud feedbacks are obtained using the radiation data set of Zhang et al. (2004). The net surface heat flux for the observations is obtained by combing the latent and sensible heat flux from the NCEP reanalysis (Kalnay et al. 1996) with the radiation data from Zhang et al. (2004). The SST data are from Rayner et al. (1996). The data for the coupled models are from a 50-year long present day control simulations by the coupled models. The model listed are: NCAR CCSM1 (Boville and Gent 1998), the NCAR CCSM2 (Kiehl and Gent 2004), the NCAR CCSM3 at T42 and T85 resolution (Collins et al. 2006), the French IPSL-CM4 (Marti et al. 2005), and the GFDL CM2 (Delworth et al. 2006). What are in the parenthesis are the corresponding results obtained from the longest corresponding AMIP runs that are available to us for these models. (The period that used for the calculation of the feedback from AMIP runs are respectively Feb. 1979—Jan. 1993 for CCSM1, January 1950—December 1999 for CCSM2, January 1979—December 1999 for CCSM3-T42, January 1979—December 2000 for CCSM3-T85, January 1979—December 1995 for UKMO HadCM3, January 1979—December 2002 for IPSL-CM4, and January 1983—Dec. 1998 for GFDL CM2.0).

Table II: Same as for Table 1, except for the 20th century simulation runs for different models from the CMIP3 Archive. The period for the simulations by all models is the same as the period covered by ISCCP data (July 1983—Dec. 2004). The names of the groups where these model runs originated, and other details about the models listed here, such as spatial resolution, type of physical package for radiation and convection, can be found at http://www-pcmdi.llnl.gov/ipcc/model_documentation/ipcc_model_documentation.php. The numbers in red are the results from the corresponding AMIP runs over the same period. Note that not all the model groups have their AMIP runs submitted. Some submitted AMIP runs do not have all the data that their corresponding coupled runs have.

Atmospheric Feedbacks in Models and Observations

Name of Process	Feedback ($Wm^{-2}K^{-1}$)							
	$\frac{\partial(G_a)}{\partial T}$	$\frac{\partial(C_L)}{\partial T}$	$\frac{\partial(G_a+C_L)}{\partial T}$	$\frac{\partial(C_S)}{\partial T}$	$\frac{\partial(C_L+C_S)}{\partial T}$	$\frac{\partial(D_a)}{\partial T}$	$\frac{\partial(F_A)^*}{\partial T}$	$\frac{\partial(F_S)}{\partial T}$
Observation	6.82±0.25	12.84±0.48	19.66±0.61	-14.05±0.72	-1.21±0.37	-21.26±1.06	-15.66±1.09	-22.66±1.08
NCAR CCSM1	8.47±0.13 (9.86±0.29)	10.89±0.34 (16.17±0.88)	19.36±0.45 (26.03±1.15)	-2.57± 0.21 (-4.28±0.49)	8.31±0.23 (11.89±0.60)	-16.66±0.52 (-15.95±1.30)	0.13±0.47 (5.80±1.03)	-5.86±0.47 (-0.23±1.03)
NCAR CCSM2	8.25±0.08 (8.48±0.13)	7.21±0.15 (6.96±0.25)	15.46±0.21 (15.44±0.35)	-0.31±0.17 (1.79±0.30)	6.90±0.18 (8.74±0.35)	-15.30±0.28 (-9.86±0.49)	-0.15±0.26 (7.36±0.42)	-6.15±0.26 (1.32±0.42)
NCAR CCSM3	9.35±0.09 (9.47±0.19)	9.68±0.20 (8.73±0.36)	19.03±0.26 (18.20±0.52)	-5.39±0.38 (-1.16±0.49)	4.29±0.26 (7.57±0.39)	-17.08±0.34 (-11.89±0.72)	-3.44±0.45 (5.15±0.75)	-9.53±0.45 (-0.91±0.75)
NCAR CCSM3(T85)	9.05±0.10 (10.17±0.17)	11.35±0.34 (13.03±0.41)	20.41±0.41 (23.20±0.51)	-5.35±0.41 (-10.99±0.57)	6.01±0.24 (2.04±0.36)	-16.40±0.45 (-16.23±0.76)	-1.34±0.48 (-4.02±0.82)	-7.38±0.49 (-10.12±0.82)
UKMO HadCM3	8.89±0.11 (10.63±0.34)	6.64±0.18 (8.98±0.55)	15.54±0.29 (19.61±0.86)	-5.26±0.28 (-10.60±0.76)	1.39±0.13 (-1.62±0.36)	-12.53±0.34 (-16.58±1.17)	-2.25±0.34 (-7.57±1.23)	-8.13±0.34 (-13.41±1.23)
IPSL CM4	9.17±0.06 (9.64±0.15)	11.89±0.23 (16.20±0.49)	21.06±0.26 (25.84±0.59)	-7.73±0.27 (-13.87±0.59)	4.16±0.16 (2.33±0.29)	-17.26±0.29 (-19.50±0.64)	-3.93±0.30 (-7.53±0.63)	-9.96±0.30 (-13.50±0.63)
GFDL CM2.0	8.82±0.08 (10.01±0.21)	10.22±0.29 (17.32±0.66)	19.04±0.34 (27.33±0.81)	-6.14±0.39 (-15.43±0.82)	4.07±0.16 (1.89±0.35)	-17.17±0.41 (-21.89±1.17)	-4.28±0.49 (-9.98±1.32)	-10.25±0.50 (-15.99±1.32)

The net atmospheric feedback $\frac{\partial(F_A)}{\partial T} = \frac{\partial(G_a)}{\partial T} + \frac{\partial(C_L)}{\partial T} + \frac{\partial(C_S)}{\partial T} + \frac{\partial(D_a)}{\partial T}$

Table I: Tropical water vapor and cloud feedbacks from observations and coupled climate models. $\frac{\partial}{\partial T}G_a$, $\frac{\partial}{\partial T}C_l$, and $\frac{\partial}{\partial T}C_s$ are respectively the water vapor feedback, the feedback from the long-wave forcing of clouds, and the feedback from the short-wave forcing of clouds. The feedback from the atmospheric transport ($\frac{\partial}{\partial T}D_a$), the net atmospheric feedback ($\frac{\partial F_a}{\partial T} = \frac{\partial G_a}{\partial T} + \frac{\partial C_l}{\partial T} + \frac{\partial C_s}{\partial T} + \frac{\partial D_a}{\partial T}$), and the feedback from the net surface heat flux into the ocean ($\frac{\partial}{\partial T}F_s$) are also listed. The values for these feedbacks are obtained through a linear regression using the inter-annual variations of the SST and the corresponding fluxes over the equatorial Pacific (5^oS-5^oN, 150^oE-250^oE). The observational results for the water vapor and cloud feedbacks are obtained using the radiation data set of Zhang et al. (2004). The net surface heat flux for the observations is obtained by combing the latent and sensible heat flux from the NCEP reanalysis (Kalnay et al. 1996) with the radiation data from Zhang et al. (2004). The SST data are from Rayner et al. (1996). The data for the coupled models are from a 50-year long present day control simulations by the coupled models. The model listed are: NCAR CCSM1 (Boville and Gent 1998), the NCAR CCSM2 (Kiehl and Gent 2004), the NCAR CCSM3 at T42 and T85 resolution (Collins et al. 2006), the French IPSL-CM4 (Marti et al. 2005), and the GFDL CM2 (Delworth et al. 2006). What are in the parenthesis are the corresponding results obtained from the longest corresponding AMIP runs that are available to us for these models. (The period that used for the calculation of the feedback from AMIP runs are respectively Feb. 1979—Jan. 1993 for CCSM1, January 1950—December 1999 for CCSM2, January 1979—December 1999 for CCSM3-T42, January 1979—December 2000 for CCSM3-T85, January 1979—December 1995 for UKMO HadCM3, January 1979—December 2002 for IPSL-CM4, and January 1983—Dec. 1998 for GFDL CM2.0).

Atmospheric Feedbacks in Models and Observations

Name of Processes	Feedback ($Wm^{-2}K^{-1}$) $\frac{\partial(G_a)}{\partial T}$	$\frac{\partial(C_L)}{\partial T}$	$\frac{\partial(G_a+C_L)}{\partial T}$	$\frac{\partial(C_S)}{\partial T}$	$\frac{\partial(C_s+C_L)}{\partial T}$	$\frac{\partial(Da)}{\partial T}$	$\frac{\partial(F_A)}{\partial T}$	$\frac{\partial(F_s)}{\partial T}$
Observation	6.82±0.25	12.84±0.48	19.66±0.61	-14.05±0.72	-1.21±0.40	-21.26±1.06	-15.66±1.09	-22.66±1.08
CNRM CM3	7.97±0.10 (10.30±0.25)	8.21±0.30 (13.74±0.67)	16.18±0.40 (24.04±0.89)	-9.53± 0.48 (-20.21±0.94)	-1.32±0.27 (-6.47±0.54)	-7.67±0.48 (-10.82±1.22)	-1.03±0.56 (-6.99±1.25)	-4.71±0.49 (-8.82±1.11)
GFDL CM2.0	8.55±0.11 (10.01±0.21)	10.63±0.39 (17.30±0.66)	19.18±0.46 (27.31±0.80)	-6.59±0.56 (-15.42±0.82)	4.03±0.25 (1.88±0.34)	-17.81±0.55 (-21.87±1.16)	-5.23±0.67 (-9.98±1.32)	-11.48±0.67 (-16.00±1.38)
GFDL CM2.1	8.54±0.10 (10.34±0.20)	9.13±0.33 (15.84±0.50)	17.67±0.40 (26.18±0.65)	-4.50±0.54 (-13.29±0.62)	4.63±0.27 (2.55±0.23)	N/A N/A	N/A N/A	N/A N/A
GISS Model_e_h	7.07±0.24 N/A	0.54±0.36 N/A	7.61±0.47 N/A	1.70±0.58 N/A	2.25±0.50 N/A	N/A N/A	N/A N/A	N/A N/A
IAP FGOALS	7.84±0.04 N/A	7.22±0.13 N/A	15.16±0.16 N/A	-2.25±0.12 N/A	5.08±0.08 N/A	-12.55±0.23 N/A	0.36±0.20 N/A	-6.11±0.20 N/A
IPSL CM4	9.40±0.11 (9.66±0.15)	13.07±0.46 (16.26±0.50)	22.47±0.51 (25.92±0.59)	-9.56±0.54 (-13.94±0.62)	3.51±0.33 (2.32±0.33)	-18.09±0.60 (-19.52±0.65)	-5.18±0.61 (-7.53±0.65)	-11.66±0.59 (-13.63±0.64)
MIROC3.2 Medres	6.69±0.16 (7.30±0.13)	8.29±0.37 (11.98±0.36)	14.99±0.49 (19.27±0.46)	-2.01±0.62 (-4.28±0.48)	6.29±0.43 (7.70±0.34)	N/A (-27.96±0.73)	N/A (-12.97±0.80)	N/A (-18.18±0.74)
MIROC Hires	7.47±0.20 (7.99±0.13)	8.76±0.52 (10.58±0.36)	16.23±0.68 (18.58±0.46)	-1.32±0.56 (-4.21±0.46)	7.45±0.30 (6.38±0.24)	-18.20±0.75 (-19.93±0.69)	-3.28±0.69 (-5.57±0.74)	-8.78±0.69 (-10.56±0.68)
MPI ECHAM5	7.90±0.13 (10.56±0.25)	6.77±0.28 17.15±0.65	14.67±0.39 (27.71±0.87)	-4.37±0.44 (-20.31±1.01)	2.40±0.23 (-3.16±0.52)	-14.62±0.49 (-27.20±1.08)	-4.32±0.54 (-19.80±1.30)	-10.33±0.52 (-24.83±1.25)
NCAR CCSM3	8.95±0.15 (10.18±0.19)	10.26±0.47 (12.93±0.51)	19.21±0.57 (23.11±0.63)	-3.69±0.58 (-10.31±0.63)	6.57±0.38 (-2.62±0.42)	-8.50±0.54 (-5.39±0.80)	7.02±0.49 (7.42±0.83)	-0.32±0.51 (0.42± 0.83)
UKMO HadCM3	9.03±0.15 N/A	6.82±0.24 N/A	15.85±0.38 N/A	-5.58±0.39 N/A	1.24±0.23 N/A	-12.52±0.46 N/A	-2.25±0.49 N/A	-8.29 ±0.48 N/A
UKMO Hadgem1	5.95±0.21 (11.06±0.31)	1.95±0.19 (14.14±0.57)	7.90±0.37 (25.21±0.85)	3.80±0.44 (-14.02±0.68)	5.75±0.36 (-0.13±0.24)	-5.70±0.52 N/A	6.00±0.69 N/A	-0.39±0.67 N/A

Table II: Same as for Table 1, except for the 20th century simulation runs for different models from the CMIP3 Archive. The period for the simulations by all models is the same as the period covered by ISCCP data (July 1983—Dec. 2004). The names of the groups where these model runs originated, and other details about the models listed here, such as spatial resolution, type of physical package for radiation and convection, can be found at http://www-pcmdi.llnl.gov/ipcc/model_documentation/ipcc_model_documentation.php The numbers in the parentheses are the results from the corresponding AMIP runs over the same period. Note that not all the model groups have their AMIP runs submitted. Some submitted AMIP runs do not have all the data that their corresponding coupled runs have

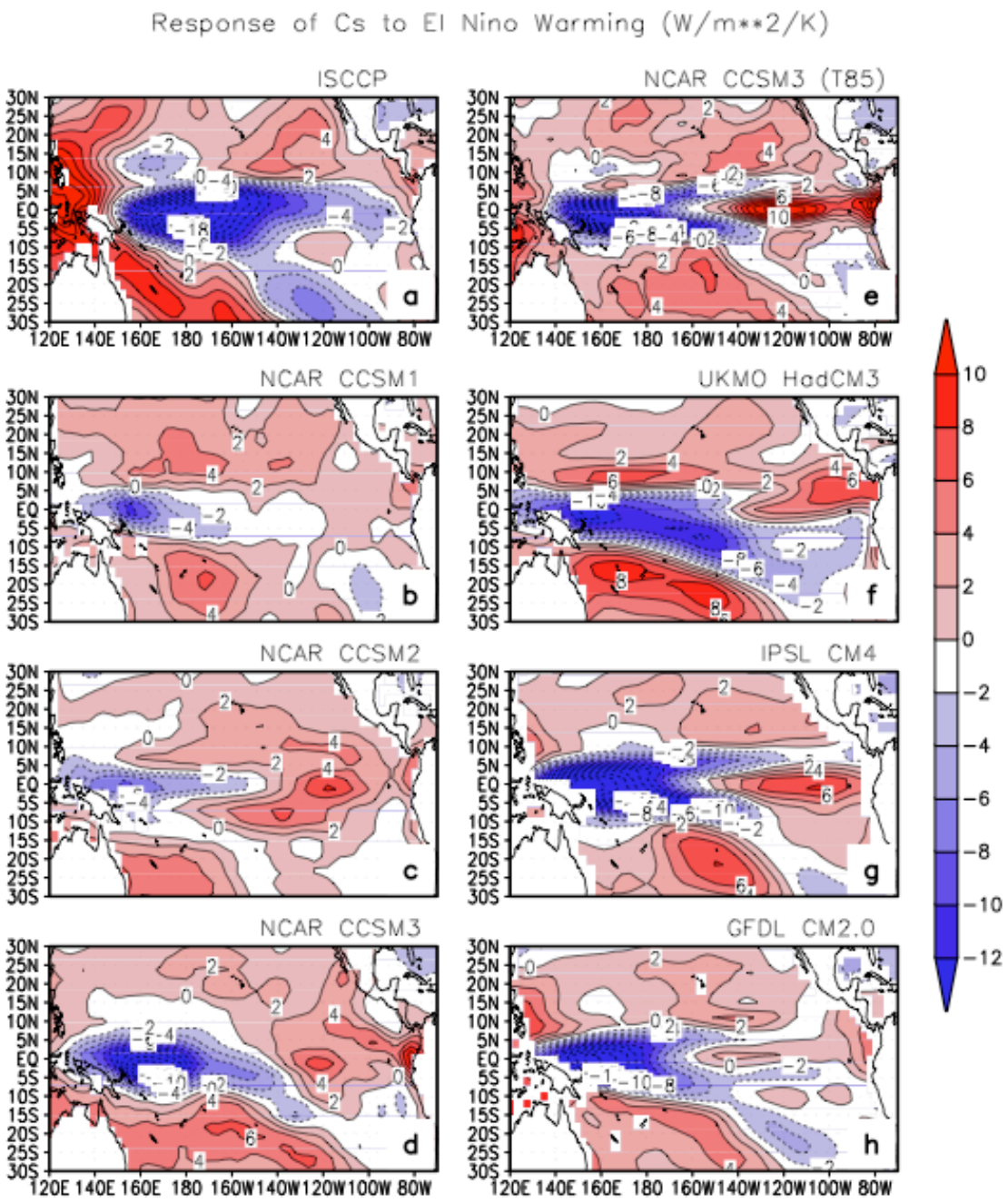

Figure 1: Response of the short-wave forcing of clouds (Cs) to El Nino warming. Shown are coefficients obtained by linearly regressing Cs at each grid point on the SST averaged over the equatorial Pacific (5°S-5°N, 150°E-250°E).

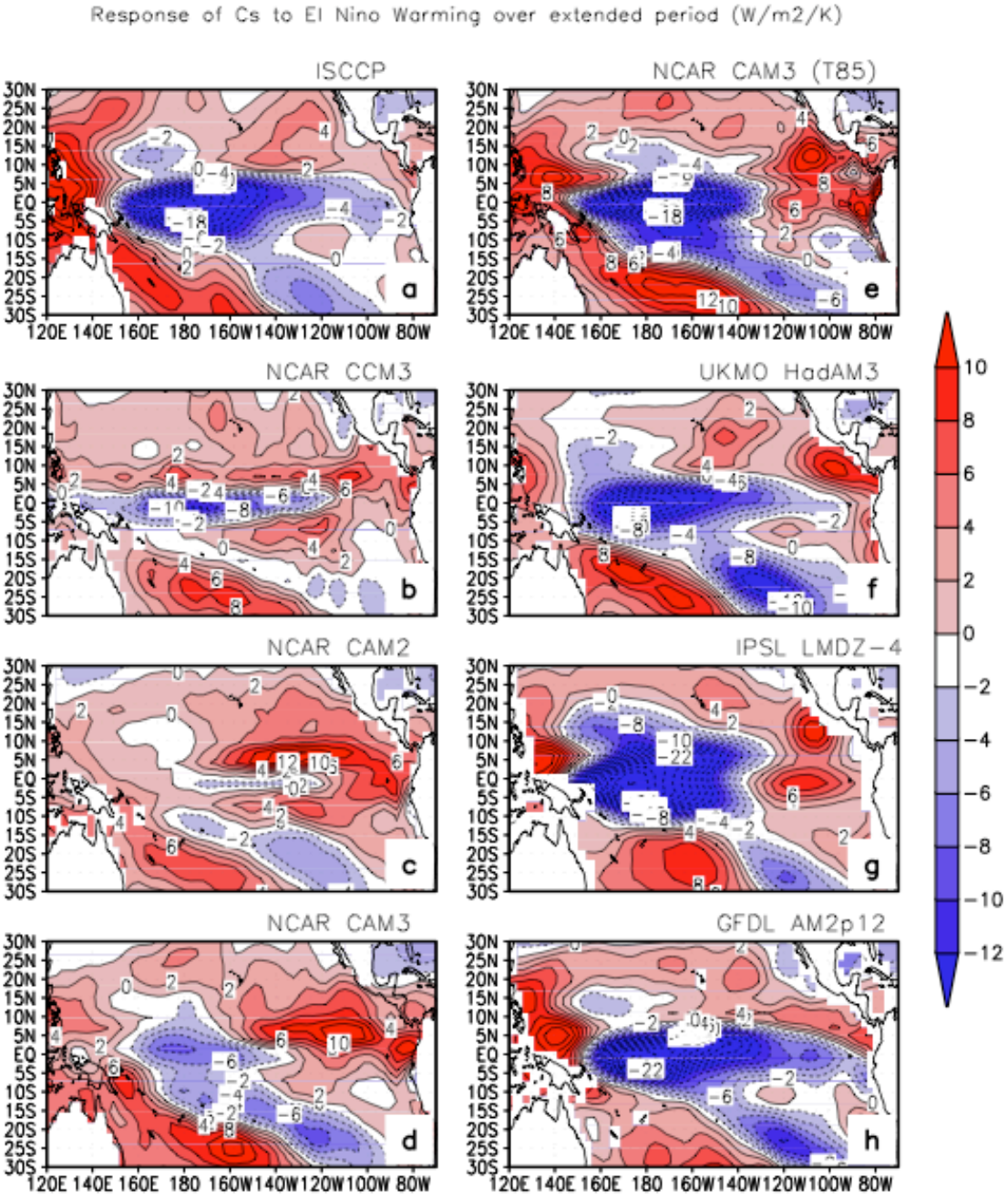

Figure 2: Same as for Fig1 except for the corresponding AMIP runs.

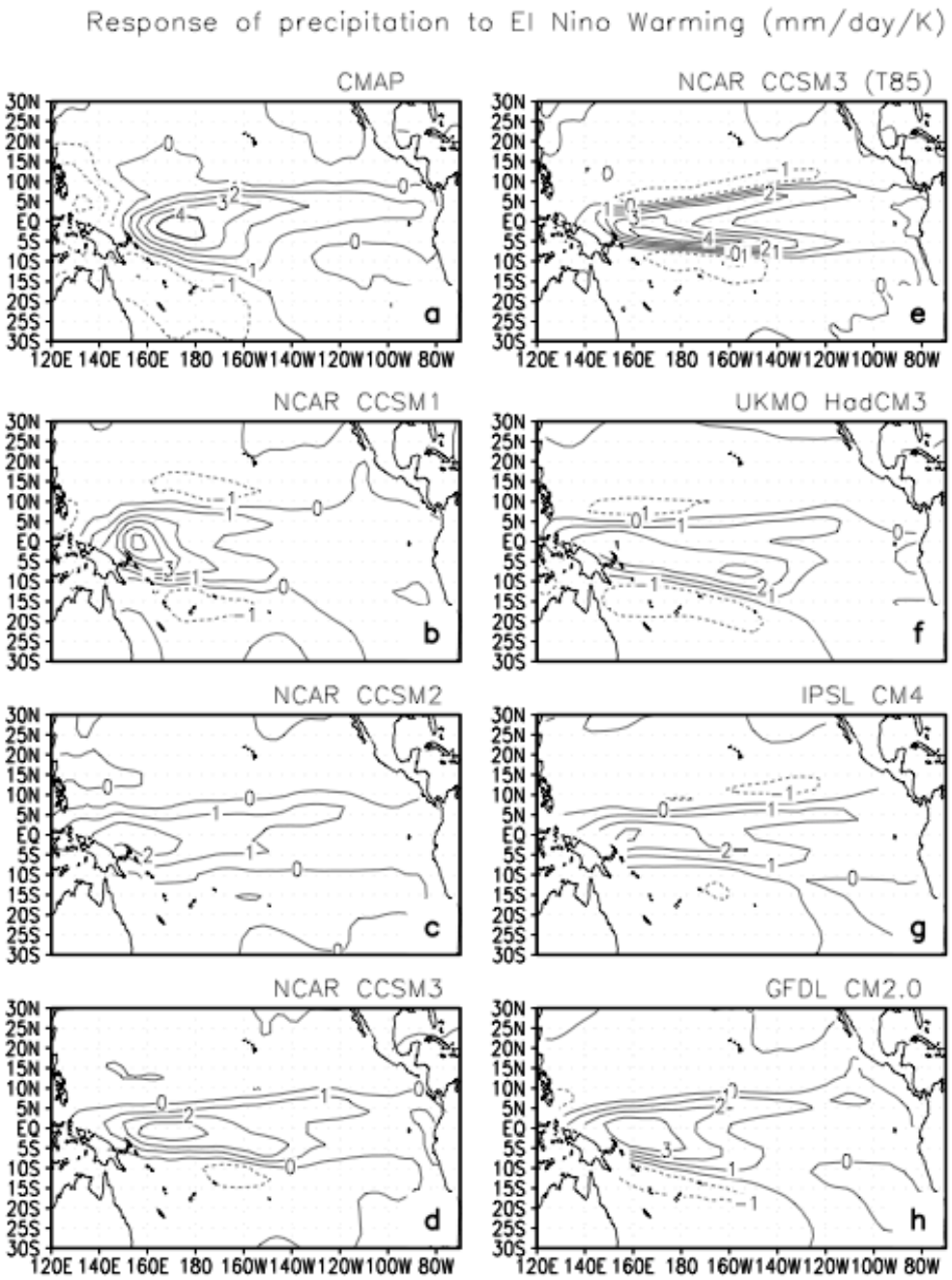

Figure 3: Same as for Fig.1, but for the precipitation. The precipitation data are from Xie and Arkin (1996).

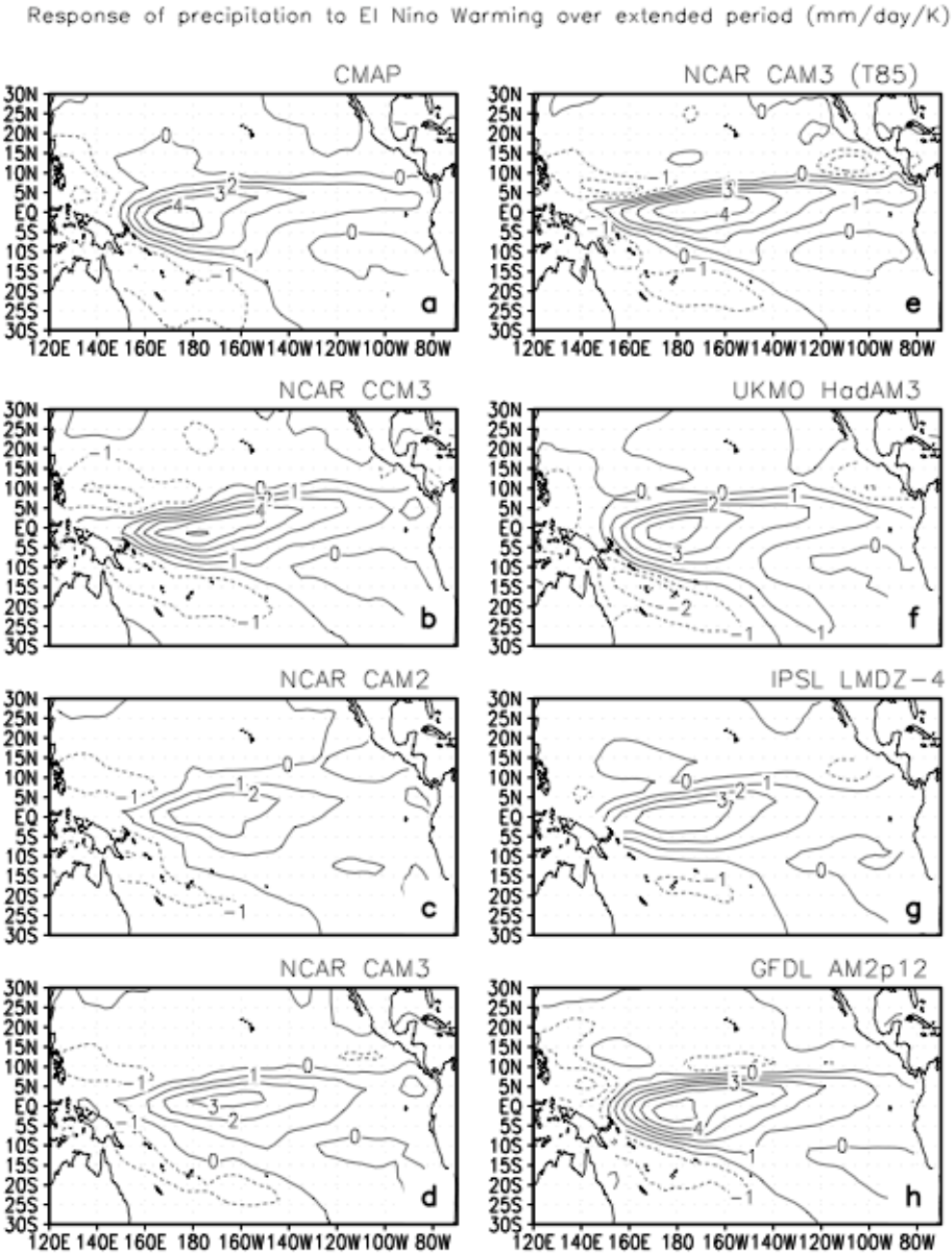

Figure 4: Same as for Fig.3 except for the corresponding AMIP runs.

(a)

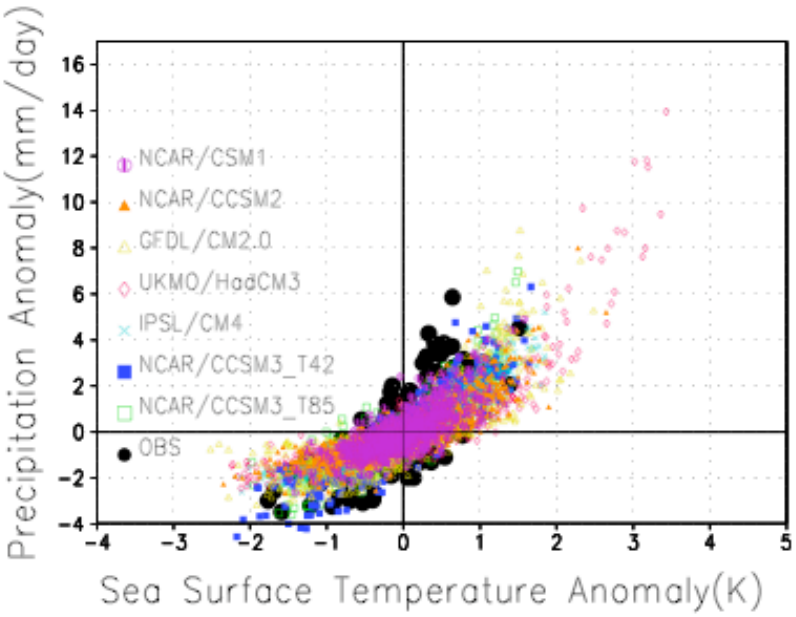

(b)

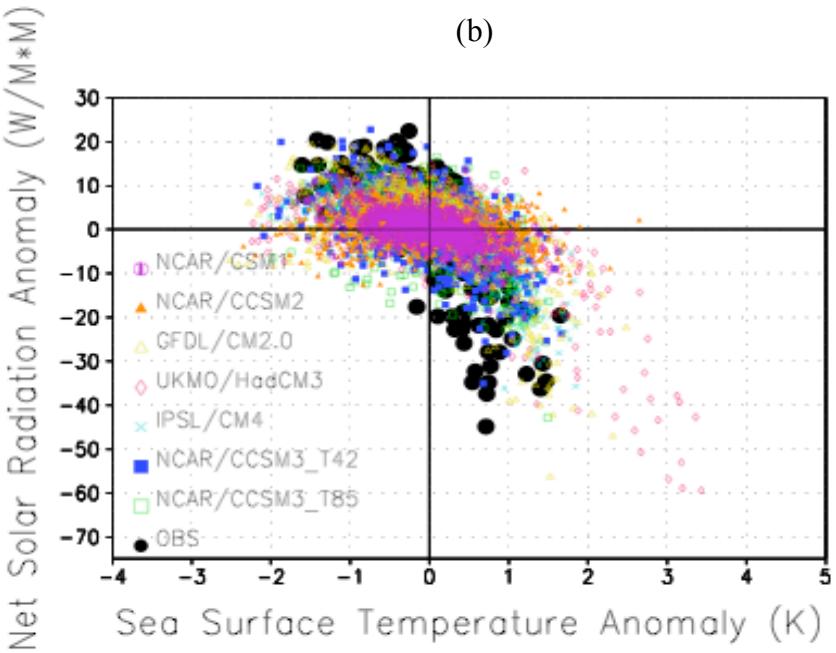

Figure 5: Scatter diagrams showing the relationship between the precipitation and the SST (a) and the relationship between the surface solar radiative heating and the SST (b) . Interannual anomalies of these quantities averaged over the equatorial Pacific (5°S-5°N, 150°E-250°E) and for the period July 1983—June 2001 are used for these figures.

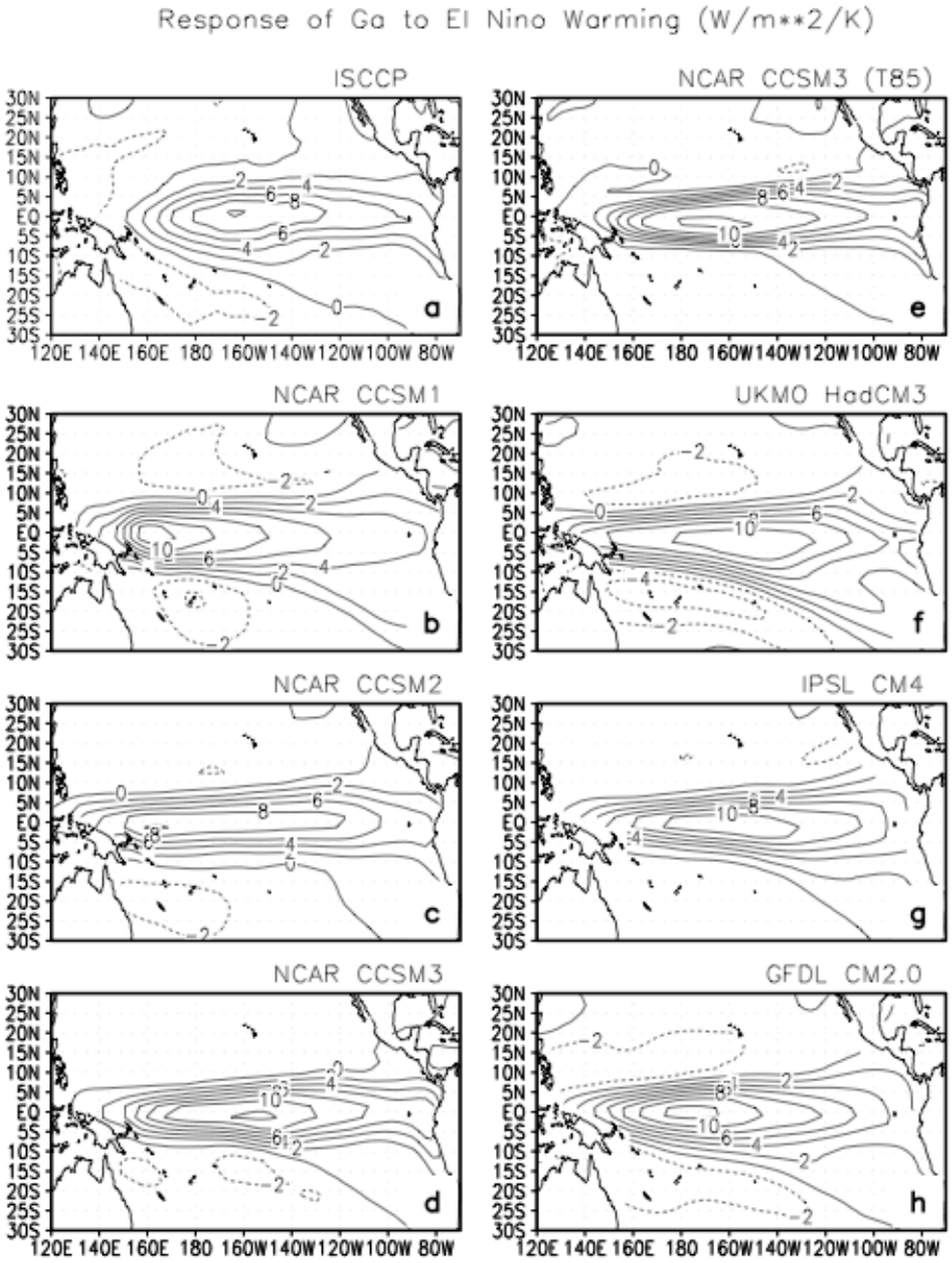

Figure 6: Same as for Fig. 1, but the greenhouse effect of water vapor (G_a).

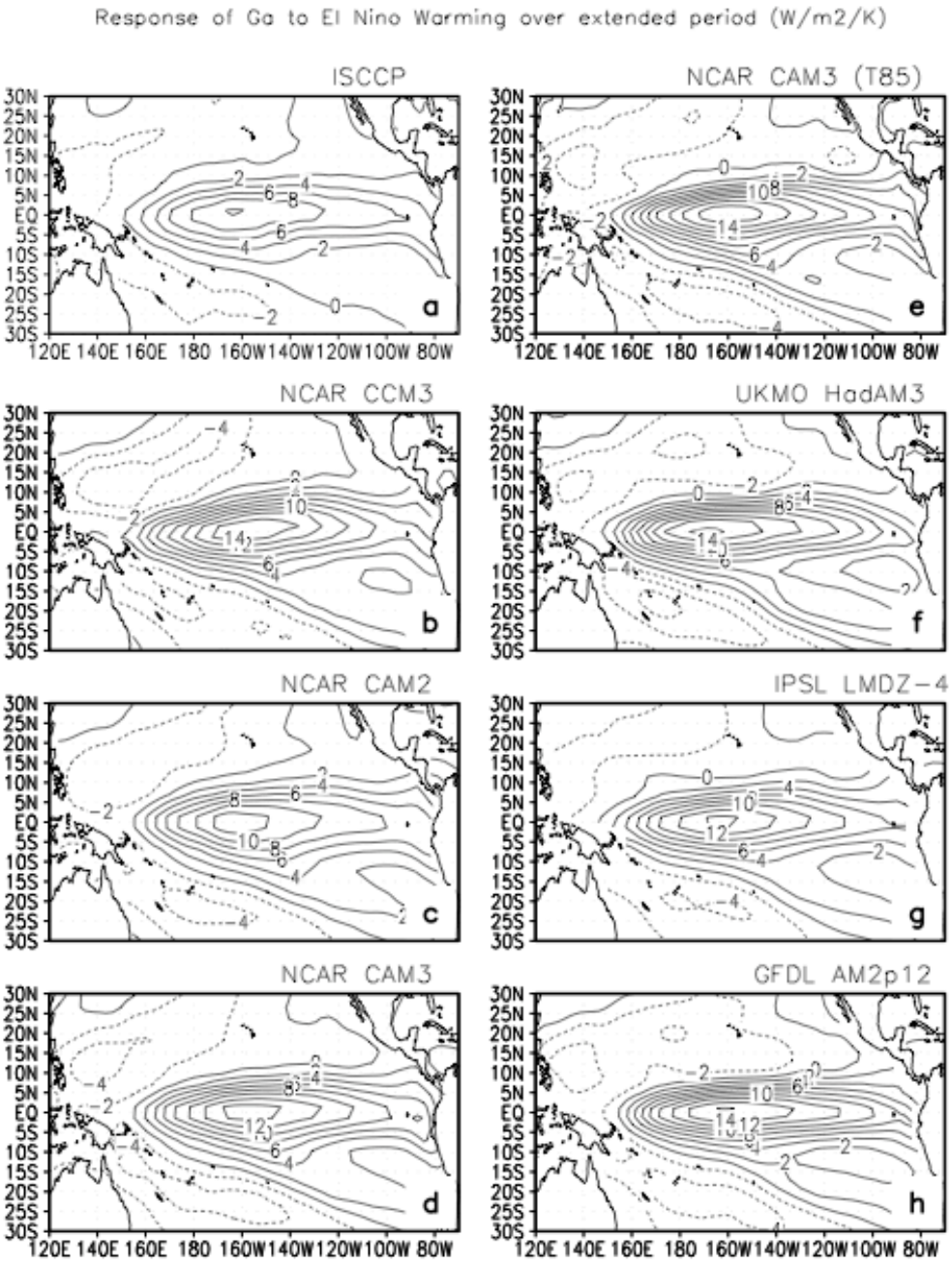

Figure 7: Same as for Fig.6 except for the corresponding AMIP runs.

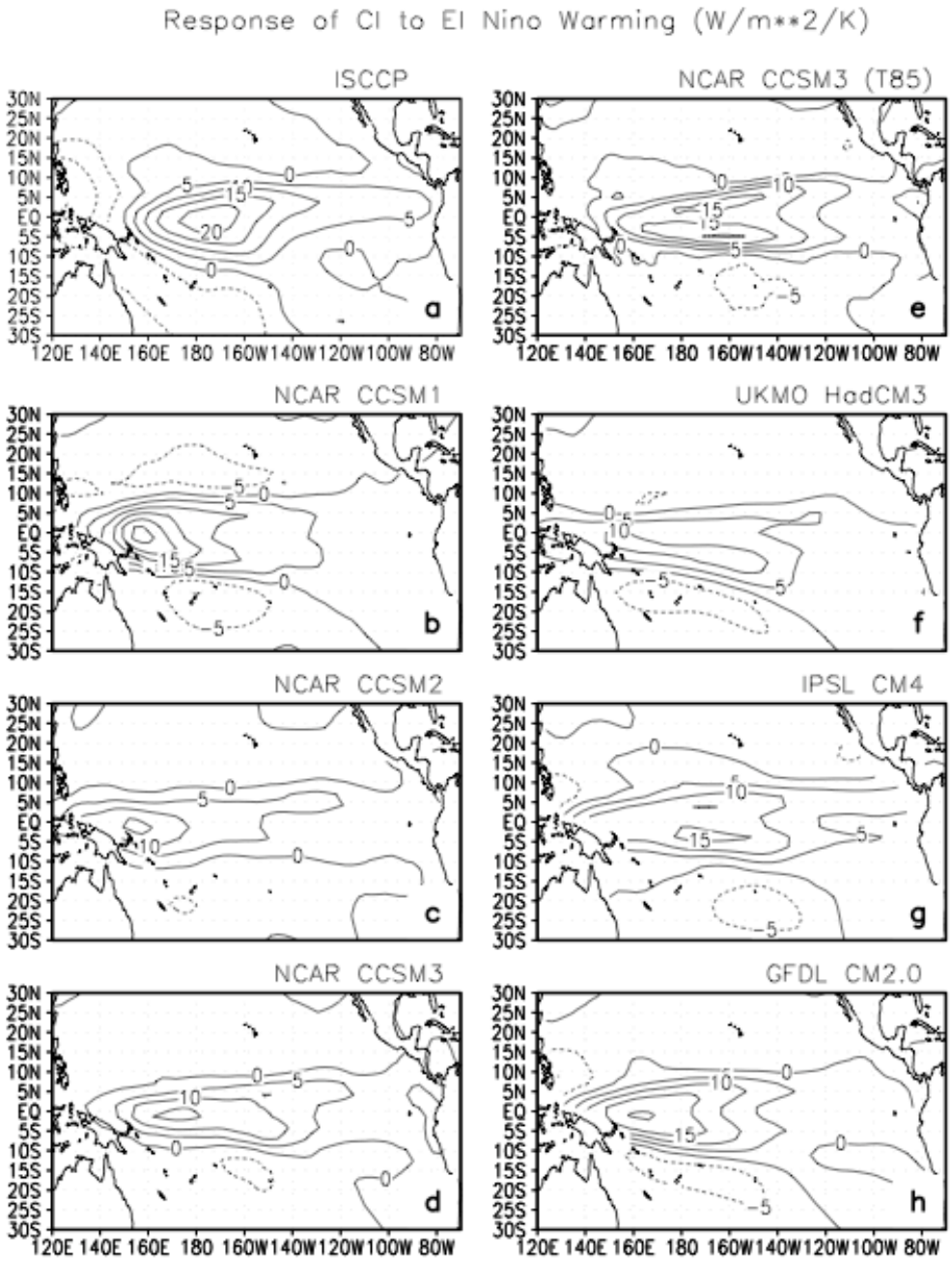

Figure 8: Same as for Fig. 1, but the greenhouse effect of clouds (C_l).

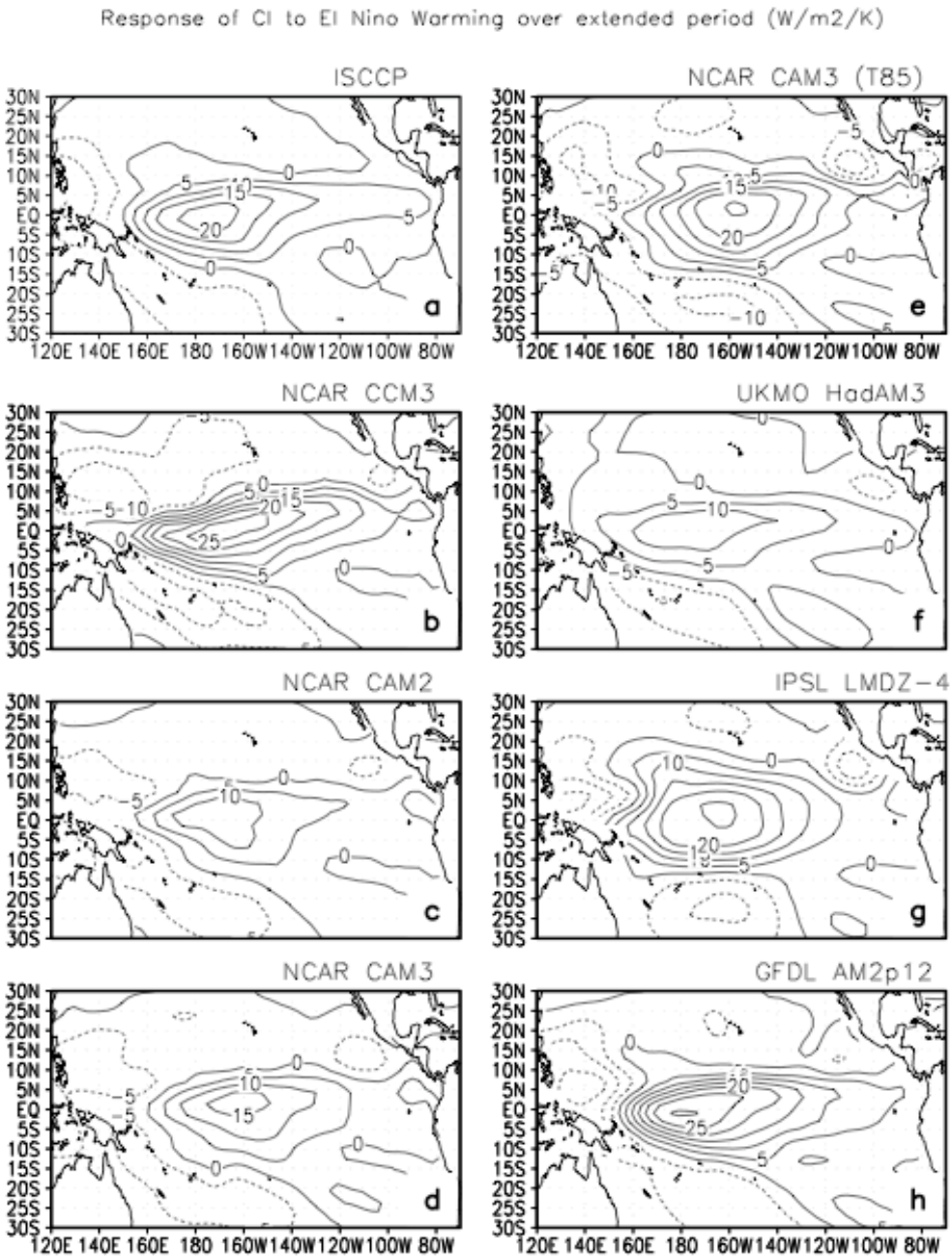

Figure 9: Same as for Fig.8 except from the corresponding AMIP runs.

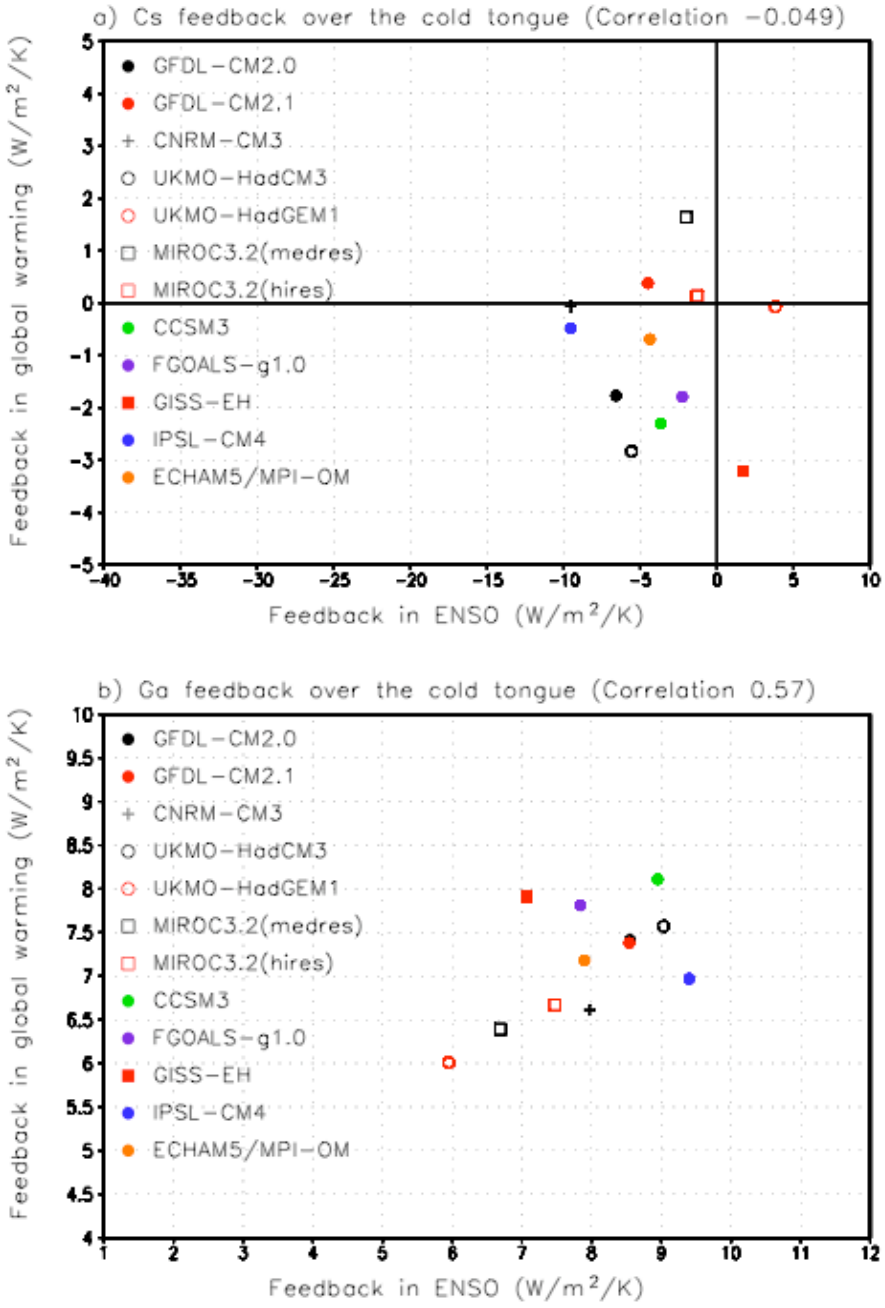

Figure 10: (a) Correlations between variations among models in the feedback from cloud albedo over the cold-tongue region during ENSO and variations among models in the same feedback during global warming over the same region. (b) Correlations between variations in the feedback from water vapor over the cold-tongue region during ENSO and the variations in the feedback during global warming over the same region. Note that the variations correlated are the variations of the concerned feedback among different models. The feedbacks in global warming were estimated from trends in the projected global warming during 2000—2100 under the A1B scenario. See text for more details.

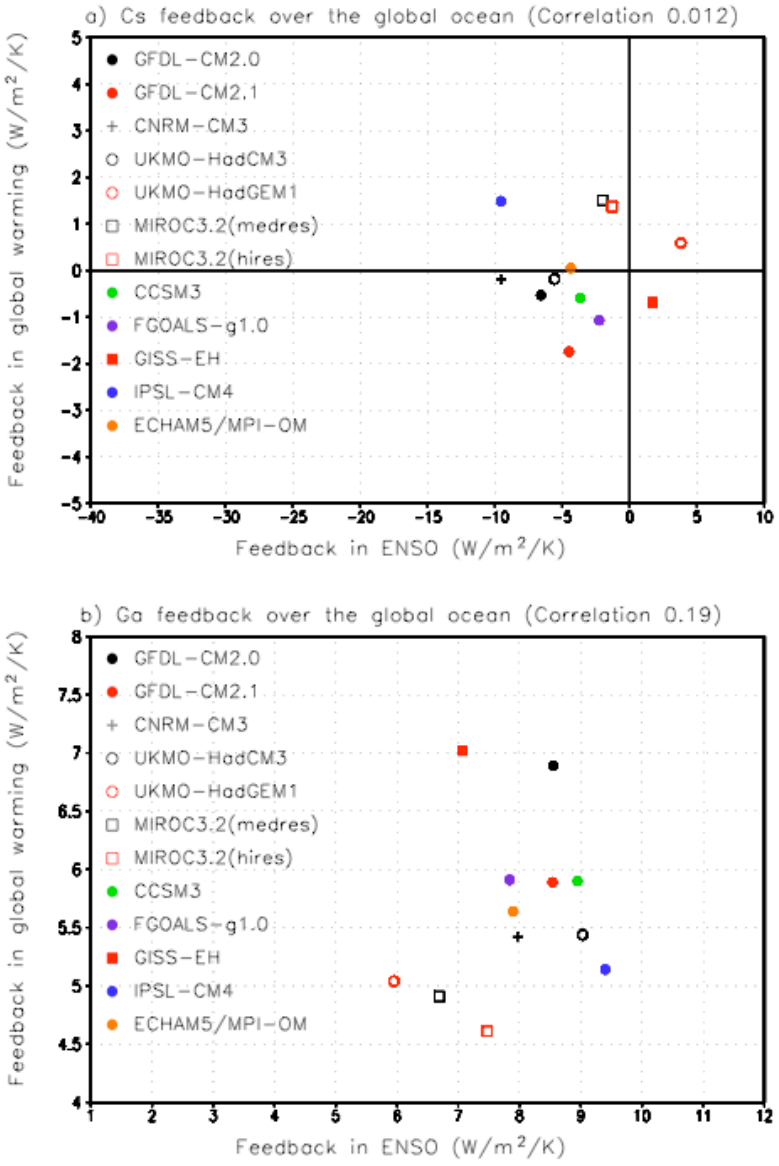

Figure 11: (a) Correlations between variations among models in the feedback from cloud albedo over the cold-tongue region during ENSO and variations among models in the same feedback during global warming over the global oceans (b) Correlations between variations among models in the feedback from water vapor over the cold-tongue region during ENSO and variations among models in the same feedback during global warming over the global oceans. The feedbacks in global warming over the global oceans were estimated from trends over the oceanic region in the projected global warming during 2000—2100 under the A1B scenario. See text more details.